Geophysical Research Letters

RESEARCH LETTER
10.1029/2025GL120522

On CMIP6 Model Consensus for the Climate Response in Eurasian Winter to Historical Volcanic Eruptions

Lisa Weber[1,2,3], **Kirstin Krüger**[4,5], **and Stephanie Fiedler**[1,2,6]

[1]University of Cologne, Institute for Geophysics and Meteorology, Cologne, Germany, [2]GEOMAR Helmholtz Centre for Ocean Research Kiel, Kiel, Germany, [3]Now at: Institute of Meteorology and Climate Research Troposphere Research (IMKTRO), Karlsruhe Institute of Technology (KIT), Karlsruhe, Germany, [4]Department of Geosciences, University of Oslo, Oslo, Norway, [5]Centre of Advanced Studies, Oslo, Norway, [6]Now at: Heidelberg University, Institute of Environmental Physics, Heidelberg, Germany

Abstract This study provides a comprehensive analysis of the climate response in Northern Hemisphere (NH) winter to major volcanic eruptions of the past, using multi-member ensembles of historical experiments of 15 models from the Coupled Model Intercomparison Project Phase 6 (CMIP6) and three reanalysis data sets. Focusing on the two largest historical eruptions of Krakatoa and Pinatubo, the results highlight a large model consensus on the strengthening of the polar vortex and an associated increase in surface temperatures over parts of Northern Eurasia in the CMIP6 multi-model mean in the first winter following the eruptions. This finding is consistent with models simulating a positive phase of the North Atlantic Oscillation (NAO). The responses of the surface temperatures and winds show hardly any dependence on the phase of the El Niño-Southern Oscillation (ENSO).

Plain Language Summary This study investigates how major volcanic eruptions influence winter climate in the Northern Hemisphere. We analyzed results from 15 climate models and reconstructed weather data to understand the typical changes following the eruptions of Pinatubo (1991) and Krakatoa (1883). The findings show that in the winters following these eruptions, the polar vortex - the strong westerly wind system high in the atmosphere over the polar regions—becomes stronger. This change is linked to higher-than-usual near-surface air temperatures across Northern Eurasia and a shift in the large-scale weather pattern over the North Atlantic, known as the North Atlantic Oscillation, toward lower sea level pressure over Iceland and higher pressure over the Azores, which favors stronger westerly surface winds and milder winters over Europe. These changes hardly depend on teleconnections from El Niño and La Niña conditions in the equatorial Pacific Ocean.

Key Points:

- Krakatoa and Pinatubo eruptions led to a stronger polar vortex and warmer surface winters over parts of northern Eurasia in the CMIP6 mean
- Internal variability affects the simulated climate responses to volcanic forcing, even in the case of strong eruptions
- CMIP6 multi-model mean shows a positive NAO phase in the first winter after the eruptions independent of the ENSO phase

Supporting Information:

Supporting Information may be found in the online version of this article.

Correspondence to:

S. Fiedler,
stephanie.fiedler@uni-heidelberg.de

Citation:

Weber, L., Krüger, K., & Fiedler, S. (2026). On CMIP6 model consensus for the climate response in Eurasian winter to historical volcanic eruptions. *Geophysical Research Letters*, *53*, e2025GL120522. https://doi.org/10.1029/2025GL120522

Received 14 NOV 2025
Accepted 10 MAR 2026

1. Introduction

Explosive volcanic eruptions can cause surface cooling by releasing large amounts of sulfur dioxide into the stratosphere, which forms sulfate aerosols that scatter sunlight back into space (Robock, 2000). Contrary to the global surface cooling after major volcanic eruptions in the tropics, warmer winters over Europe and Asia have been observed (Robock & Mao, 1992, 1995). Robock (2000) attributes this surface winter warming to the strengthening of the NH polar vortex, which leads to a positive phase of the NAO and, therefore, higher surface temperatures across Europe. The enhancement of the polar vortex results from an increased meridional temperature gradient in the lower stratosphere due to the heating of the volcanic aerosols in the equatorial stratosphere.

Following studies suggest more complex pathways and additional mechanisms of the polar vortex response. Stenchikov et al. (2002) proposed that ozone depletion, as a consequence of the volcanic eruption in the polar region, leads to additional cooling and, hence, to further strengthening of the polar vortex. In addition, they propose a reduction of the meridional tropospheric temperature gradient leading to reduced planetary-scale wave activity and, thereby, a less disturbed polar vortex. Poberaj et al. (2011) and Toohey et al. (2014), however, found enhanced planetary wave activity and, hence, dynamically disturbed polar vortices in the Southern and Northern Hemispheres following the Pinatubo eruption.

Previous studies have analyzed the ability of climate models to reproduce the observations in historical experiments across the different phases of CMIP. Models in CMIP3 show a weak enhancement of the NH polar vortex and no winter warming over Europe (Stenchikov et al., 2006). Similarly, Driscoll et al. (2012), find no sufficient

strengthening of the NH polar vortex and no shift toward a positive NAO phase in CMIP5 models. In addition, Charlton-Perez et al. (2013) find no difference in the response to volcanic eruption between high- and low-top models of CMIP5. The sensitivity of reproducing the polar vortex response after Pinatubo was examined in MPI-ESM-LR by Toohey et al. (2014), showing that a strengthening of the polar vortex depends on the spatio-temporal structure of the forcing. Moreover, Paik et al. (2023) identify a positive annular mode after the eruptions of Krakatoa 1883 and Pinatubo 1991 based on reanalyses and CMIP6 models.

Three potential reasons for different model results in previous studies are the impact of internal variability in the NH winter stratosphere (Krüger et al., 2005; Labitzke, 1982; Labitzke & Van Loon, 1999), a dependency of responses on the strength of the volcanic forcing (Metzner et al., 2014; Schmidt & Black, 2022), and study differences in the data analysis (Azoulay et al., 2021; Polvani & Camargo, 2020). Bittner, Timmreck, et al. (2016) find variability in the polar vortex response to volcanic eruptions with magnitudes like those of Pinatubo and Krakatoa, but larger eruptions like Tambora 1815 significantly strengthened the polar vortex. In addition, only such strong eruptions produced the vortex response with a surface winter warming pattern (Bittner, Timmreck, et al., 2016; Zambri ∧ Robock, 2016). Using the 100-member ensemble of historical experiments from MPI-ESM-LR, Bittner, Schmidt, et al. (2016) indicate that more than 15 individual simulations are needed to separate a forced strengthening of the polar vortex from its internal variability. Moreover, the role of modes of internal variability in modulating the response to volcanic forcing is under discussion. Specifically, there are different results for the role of the El Niño Southern Oscillation (ENSO) in modulating the NH winter response to volcanic eruption. Coupe and Robock (2021) suggest the need for a co-occurrence of El Niño to reproduce the higher temperatures following volcanic eruptions across Europe. However, Dogar et al. (2024) find no dependency of the winter temperature response across Europe to the ENSO phase. Both Polvani et al. (2019) and Polvani and Camargo (2020) argue that the observed surface winter warming following the eruptions of Krakatoa and Pinatubo is indistinguishable from the large internal variability of the NH polar vortex strength and surface temperatures across Eurasia. The required strength of an idealized volcanic forcing in MPI-ESM-LR is 2.5–5 Tg (S) (magnitude between Agung 1963 and El Chichon 1982) for the polar vortex response and more than 10 Tg(S) (stronger than Pinatubo 1991-Krakatoa 1883) for the surface winter warming over Northern Eurasia (Azoulay et al., 2021). These studies have also used different areas for computing the temperature response, namely Eurasia (Polvani & Camargo, 2020) and Northern parts of Eurasia only (Azoulay et al., 2021).

These ongoing discussions underscore the need to revisit the Northern Hemisphere and European winter climate response to major volcanic eruptions. Both a sufficiently strong eruption and a large enough ensemble size to account for the large atmospheric variability seem to be key for simulating a significant response. Therefore, this work examines the response of the stratospheric polar vortex in the NH winter after the two largest volcanic eruptions, Krakatoa and Pinatubo, across CMIP6 historical experiments with each at least 10 ensemble members and three reanalyses to account for both model-to-model differences and internal variability of atmospheric dynamics. The focus is on testing the hypothesis that the response to the stratospheric aerosols from volcanic eruptions depends on the ENSO phase and favors a strengthened polar vortex, positive NAO index, and higher winter temperatures across Northern Europe.

2. Data and Methods

We use monthly mean output from 15 CMIP6 models, which have at least 10 ensemble members for the historical simulations for 1850–2014 with details listed in Table S1 of Supporting Information S1. The models use the prescribed stratospheric aerosol data set for CMIP6 by Thomason et al. (2018). We assume no difference between high-top and low-top models (simulated atmospheric height below 1 hPa) in our analysis, since Charlton-Perez et al. (2013) and Paik et al. (2023) show similar results for high- and low-top models in CMIP. Further, three Reanalysis Products (20CRv3 (Slivinski et al., 2019), ERA5 (Hersbach et al., 2020), and JRA-55 (Kobayashi et al., 2015)) are used to compare the climate impact of volcanic eruptions in the historical period (Table S2 in Supporting Information S1).

We interpolated the data for temperature, winds, and sea level pressure to a common horizontal grid with a resolution of 192 × 96 grid cells in longitude and latitude. A second-order conservative remapping in spherical coordinates was applied (Jones, 1999). An ensemble mean across the realizations from each model was calculated before averaging these 15 model means for the CMIP6 multi-model mean. Our multi-model means are therefore multi-model multi-realization averages.

The zonal and spatial anomalies for the first winter after the two volcanic eruptions were calculated relative to the mean over the five NH winters (DJF) prior to the eruption, following earlier studies (e.g., Stenchikov et al., 2002; Zambri & Robock, 2016). Specifically, the NH winter after the August 1883 eruption of Krakatoa, DJF 1883/84, is compared against NH winter of 1878/79–1882/83, and the winter after the June 1991 Pinatubo eruption DJF 1991/92 is compared against NH winter of 1986/87–1990/91. The averaged anomalies across the two volcanic eruptions were combined into a composite of the responses. To assess the winter surface warming over Eurasia, the mean over two regions was computed, 40–70°N and 0–150°E as in Polvani and Camargo (2020), and 55–80°N and 10–90°E as in Azoulay et al. (2021). The polar vortex strength was assessed at 60°N at 10 hPa as in Polvani and Camargo (2020).

The principal-component-based NAO-Index is calculated for each ensemble member for each NH winter using the mean sea level pressure anomalies of the Atlantic region 20–80°N, 90°W–40°E (Hurrell et al., 2003). The anomalies in NAO are calculated with respect to the 30-year moving mean for each realization separately prior to averaging across the multi-model multi-realization ensemble. The calculation of the Empirical orthogonal function (EOF) is done by using the eofs-Library (Dawson, 2016). Multi-realization averages of EOF1 per model are shown in Figure S1 of Supporting Information S1. For the ENSO phase, we computed the Oceanic Niño Index (ONI) (NOAA classification; www.climate.gov/news-features/understanding-climate/climate-variability-oceanic-nino-index, last access: 24 September 2025) following Vecchi and Soden (2007) and Khodri et al. (2017) based on relative sea surface temperature (rSST). To eliminate the mean volcanic cooling after the eruption, we subtract the tropical mean, computed as spatial average of SSTs between 20°S and 20°N, at each grid point prior to computing ONI. The ONI is the rolling 3-month average temperature anomaly of these residual rSSTs over the Niño 3.4 region covering 5°N–5°S and 170–120°W. ONI of +0.5 or higher indicate El Niño and −0.5 or lower La Niña.

3. Results and Discussion

3.1. Global Mean

The CMIP6 multi-model mean reproduces the expected climate responses in the global mean following major volcanic eruptions between 1850 and 2014. Volcanic eruptions lead to an increase of the global mean aerosol optical depth of 0.1–0.2 (Figure 1). Averaged across the models, we quantify a consistent increase in the global means of the top-of-atmosphere outgoing shortwave radiation of 1–3 Wm^{-2} and of the lower-stratosphere temperature of 1 K–3 K, while the global mean surface temperature decreases by up to 0.27 K, which is similar in CMIP3 (Stenchikov et al., 2006) and CMIP5 (Driscoll et al., 2012). The magnitude of the global mean cooling following the eruption of Pinatubo in the CMIP6 mean of −0.18 K agrees well with the three reanalysis data set assessed here (Figure 1d), consistent with Pauling et al. (2023).

Internal variability strongly affects simulated anomalies in the surface temperature and atmospheric circulation patterns to volcanic forcings. In Figures 1e–1g, the average across CMIP6 for each winter is marked for zonal winds surrounding the polar vortex (60°N at 10 hPa), NAO indices, and surface temperature across Northern Europe. In the CMIP6 multi-model mean, a strengthened polar vortex in the winter after volcanic eruptions can be seen, especially for the strong eruptions of Pinatubo and Krakatoa (Figure 1e). This tendency is also reflected in a mean positive NAO-Index (Figure 1f), although the mean NAO-Index is negative in the winter after the eruption of Agung and has values of similar magnitude in some winters without preceding volcanic activity, for example, in the 1940s. For the spatially averaged wintertime surface warming in Northern Europe (Figure 1g), the CMIP6 mean shows a strong response for the strongest volcanic eruption of Krakatoa. The eruption of Pinatubo and smaller eruptions induce magnitudes of the mean surface warming in winter that fall within the variability for wintertime temperature anomalies across the historical period. A strengthened polar vortex, therefore, does not necessarily lead to surface warming in post-eruption winters in Northern Europe, due to the internal variability of atmospheric dynamics. This variability in the post-eruption winters is also apparent for the polar vortex strength and surface temperature in Northern Europe in individual CMIP6 models with some showing increases while other ones decreases after volcanic eruptions (see Figure 4). Moreover, the time series reveal that the largest response to volcanic forcings occurs in the first winter after the eruptions and is most pronounced for Krakatoa and Pinatubo, for example, consistent with Bittner, Schmidt, et al. (2016), Zambri and Robock (2016). In the following analyses, we therefore focus on the response in the first winter after these two eruptions.

10.1029/2025GL120522

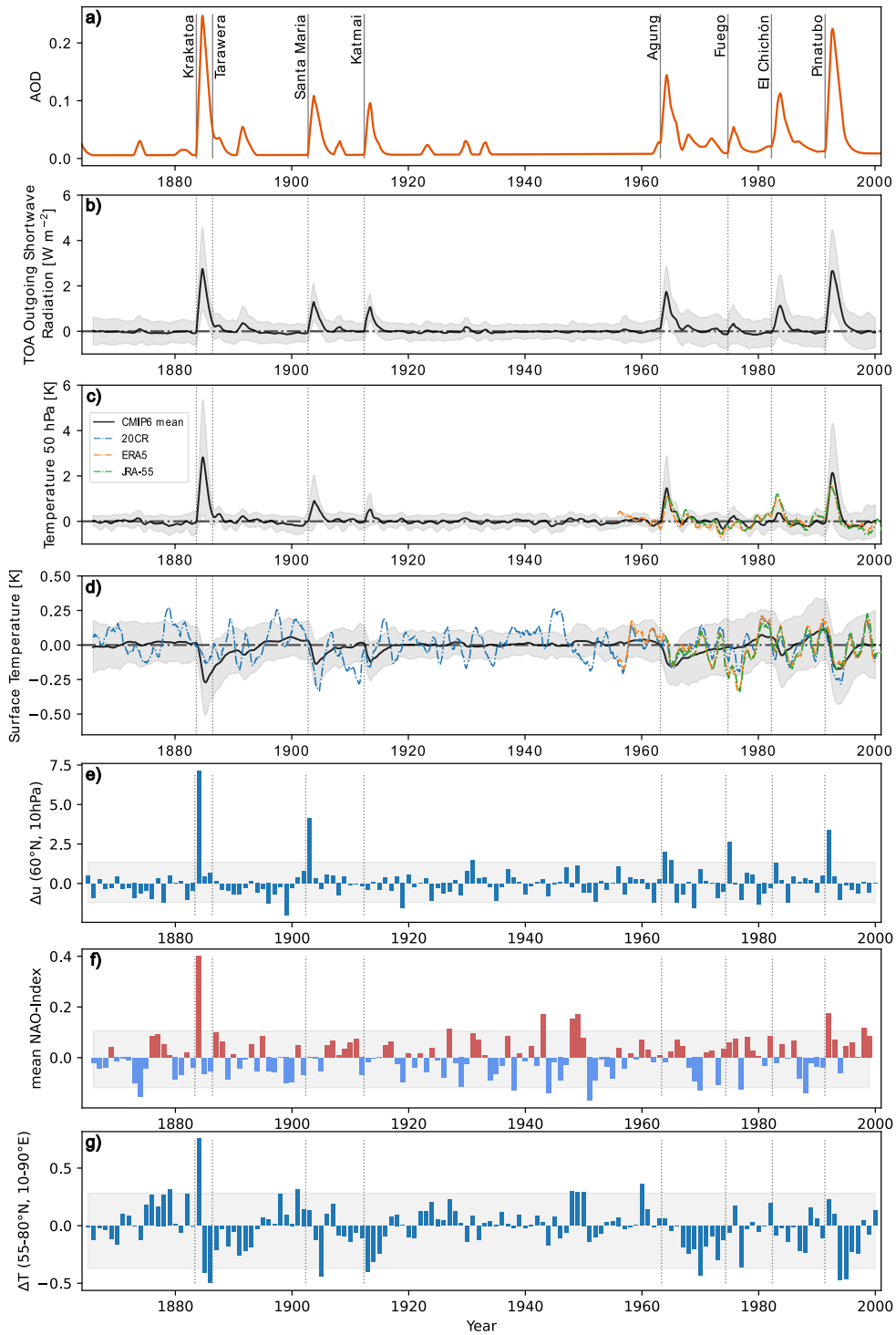

Figure 1. Time series of spatially averaged responses as simulated by the CMIP6 historical experiments. Shown are (a) stratospheric AOD of CMIP6 forcing data in orange (Thomason et al., 2018), (b–d): multi-model means of (b) top-of-atmosphere (TOA) Outgoing Shortwave Radiation, (c) Temperature anomaly at 50 hPa, and (d) Temperature anomaly at the surface. (b–d): Shading in panels (b–d) marks twice the standard deviation between the means of individual models, black is the CMIP6 multi-model mean, and colors following the legend in c are different reanalysis products. Values in panels (a–d) are deseasonalized and detrended using a 30-year moving median and shown as 12-month running means. Panels (e–g): the CMIP6 multi-model mean for NH winter (December to February) of (e) zonal wind anomalies Δu in the polar vortex (60°N at 10 hPa), (f) NAO-Index and (g) ΔT over Northern Europe (55–80°N and 10–90°E). Values for the winters are computed with a 30-year moving median such that the time axis covers 1865–1999. Shaded areas in panels (e–g) mark the 5th to 95th-percentile range of the mean across winters in the CMIP6 historical experiments for 1865–1999 inclusive. Vertical gray lines in panels (a–g) mark the time of volcanic eruptions with names listed in panel (a).

3.2. Spatial Patterns

The CMIP6 multi-model mean for the first winter following the two strongest eruptions exhibits the expected anomaly patterns for zonal wind, temperature, surface temperature, and sea level pressure with model consensus at some but not all latitudes and heights (Figure 2). Specifically, the warming of the tropical lower stratosphere is consistent for most CMIP6 models, with an average heating of up to 5.2 K (Figure 2a). For most of the troposphere, a cooling occurs, especially in the tropics, maximizing up to −0.8 K near the surface with large model consensus (Figure 2c). Toward high latitudes, CMIP6 model consensus appears for a lower stratospheric cooling paired with stratospheric warming aloft. Northern Eurasia shows the expected surface winter warming pattern with an average warming of up to 1.25 K in the CMIP6 multi-model mean (Figure 2c), although not all models agree on the sign of temperature responses to volcanic forcing in the mid-latitudes.

The strengthening of the NH polar vortex is largely consistent across CMIP6 models with an increase in zonally averaged zonal winds of up to 5.23 ms^{-1} in the CMIP6 mean at 60°N around 10 hPa (Figure 2b). Model consensus is also seen for the reduction of the SH summer easterlies in the tropical stratosphere of up to 8.2 m^{-1} and the subtropical jet in the NH of up to 2.8 m^{-1} is simulated, similar to the response in Toohey et al. (2014). Consistently, the mean-sea level pressure response shows the pattern of a positive NAO phase, with an increase in the pressure difference between the Icelandic low and the Azores high of around 3 hPa (Figure 2d).

We evaluate the degree of consensus of CMIP6 simulated responses by computing the number of models that agree on a significant response of temperatures and zonal winds (Figure 3). Almost all models show a significant warming of the tropical lower stratosphere, cooling across the tropical troposphere, reductions of the SH summer easterlies in the stratosphere and of the subtropical jet in the NH in the winter after the two eruptions (Figures 3a and 3b). Moreover, 11 of 15 models show a significant strengthening of the polar vortex (Figure 3b). The model consensus on significant responses is typically smaller at surface level compared to higher altitudes, for example, only some models show significant changes in the sea level pressure pattern in the North Atlantic and in the surface winter warming in parts of Eurasia (Figures 3c and 3d).

Past analyses of the CMIP5 models concluded that models do not reproduce a strengthening of the polar vortex (Charlton-Perez et al., 2013; Driscoll et al., 2012), but assessing the response in the first winter after strong volcanic eruptions might be important to separate the forced response from internal variability (Bittner, Timmreck, et al., 2016; Zambri & Robock, 2016). Indeed, the CMIP6 multi-model mean using at least ten-member ensembles of individual historical experiments shows the Eurasian surface warming response in the first winter after the volcanic eruptions assessed here (Figures 3c and 3d). The simulated anomaly in sea level pressure captures the observed and expected patterns and, compared to the CMIP5 model mean by Zambri and Robock (2016), the pressure in the Azores High increases in the CMIP6 mean. Hence, our analysis also shows a positive NAO in winters after eruptions, which is independent of the individual CMIP6 models in line with Paik et al. (2023).

3.3. Internal Variability

Internal variability influences the NH stratospheric polar vortex and the surface temperature across Europe. For illustrating the influence in attributing the climate response to volcanic forcing, we examine the response in individual CMIP6 historical experiments in Figure 4. For the two strong volcanic eruptions in the historical period, the variability of the polar vortex strength is clearly evident with most models indicating stronger westerly winds in the polar vortex (at 10 hPa, 60°N). The multi-model means indicate that the wind speed in the polar vortex scales with the strength of the eruption, with stronger winds following the Krakatoa eruption compared to Pinatubo (Figures 4a–4d).

Differences among the analyzed models are apparent, with varying numbers of models showing significant regional anomalies. While the forced heating of the lower tropical stratosphere in the first winter after the volcanic eruptions is captured in almost all models, the strengthening of stratospheric zonal mean wind in the NH is simulated by fewer models, and associated changes in sea level pressure and surface temperatures in Eurasia in even less models (compare Figures 3a–3d). Due to the influence of large internal variability during NH winter, we do not expect the forced near-surface warm anomaly to occur over the same Euroasian domain in all individual model realizations and in reanalysis data (compare Figure S2 in Supporting Information S1). For the same reason the location of the surface winter warm anomaly can differ between observational data and models (Graf

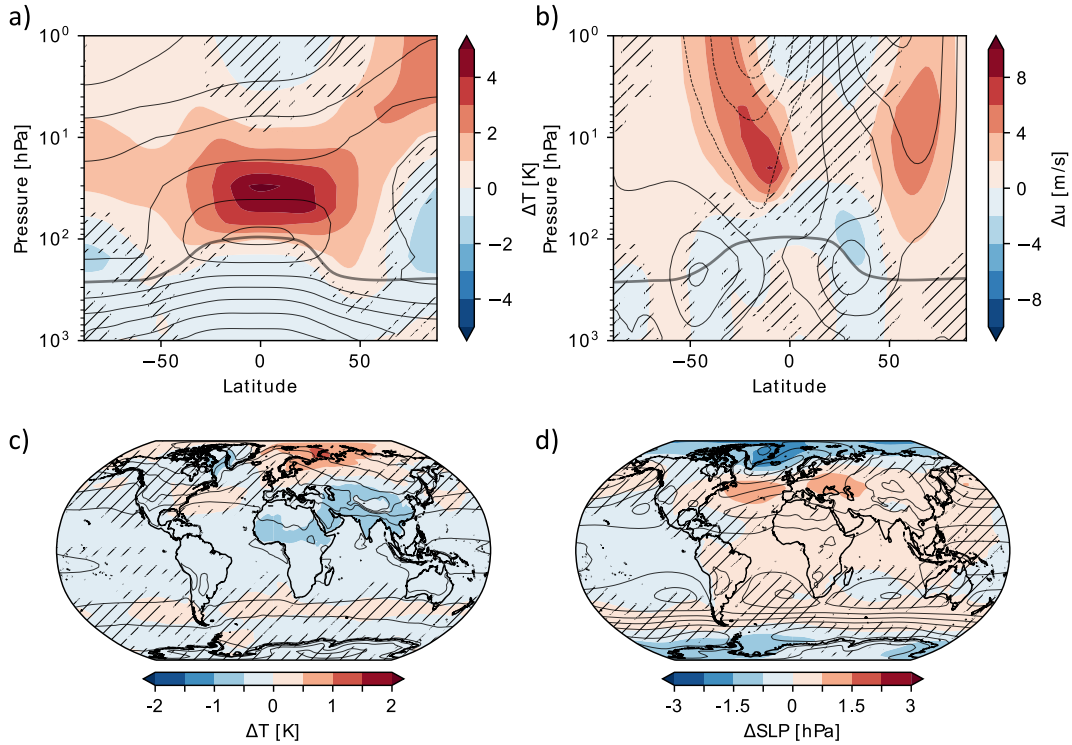

Figure 2. Composite CMIP6 multi-model mean for NH winter after the Krakatoa and Pinatubo eruptions. Shown are mean anomalies of (a) zonal temperature, (b) zonal wind, (c) surface temperature, and (d) sea level pressure averaged across all models and the two eruptions in shading. Areas with less than 70% of the models agreeing on the sign of the anomaly are hatched. Gray contours are isolines for the mean over the five winters before the eruptions with (a) 15 K, (b) 15 m^{-1}, (c) 10 K, (d) 6 hPa increments. The mean topopause height from CNRM-ESM2-1, IPSL-CM6A-LR, UKESM1-0-LL, GISS-E2-1-G and CESM2 for NH winter 1986–1991 is marked with a thick gray line in panels (a, b).

et al., 2014; Paik et al., 2023), quite apart from potential simulation biases in processes like the stratospheric polar vortex (Rao et al., 2022) and tropospheric dynamics, for example, mid-latitude storm tracks (Schemm, 2023), that both impact near-surface weather.

The area for quantifying the spatial mean is particularly relevant for the Eurasian temperature response to the extent that choosing a different regional average - as was done in past studies - can suppress the temperature response from CMIP6 (see Figures 4a–4d). Using the Eurasian box, as defined by Polvani et al. (2019), no clear surface winter warming signal is seen. Using the box across Northern Eurasia as in Azoulay et al. (2021) shows a surface warming in the CMIP6 multi-model mean. Nevertheless, the surface temperature response is variable across individual historical experiment underlining the need for large ensembles to quantify the response. Many ten-member ensembles of individual models show the stronger polar vortex paired with a winter near-surface warming in Eurasia, with only few exceptions like INM-CM5-0 and MIROC-ES2L (see Figure S3 in Supporting Information S1).

A positive NAO-Index after the two eruptions is visible in many historical experiments (color-coded in Figures 4a–4d). Half of the individual ensemble members have a positive NAO-Index of more than 0.5 for the winter after the Krakatoa eruption paired with a stronger polar vortex and Eurasian near-surface warming, seen as model responses in the upper right quadrants of Figures 4a–4d. Most but not all individual model realizations tend to a positive NAO in post-eruption winters that fall at the upper end of the distribution of NAO indices arising from internal variability of the atmosphere (Figure S4–S5 in Supporting Information S1). Our NAO results are consistent with the stratospheric pathway for the dynamics response to volcanic forcing (Bittner, Timmreck, et al., 2016; Robock, 2000; Stenchikov et al., 2002), namely an enhanced meridional temperature gradient in the lower stratosphere leading to a stronger polar vortex, and pressure changes in the troposphere that are characteristic for a positive NAO. Polvani et al. (2019), Polvani and Camargo (2020) questioned the relationship between the observed winter anomalies and the role of the volcanic eruptions, as the large variability of the NH

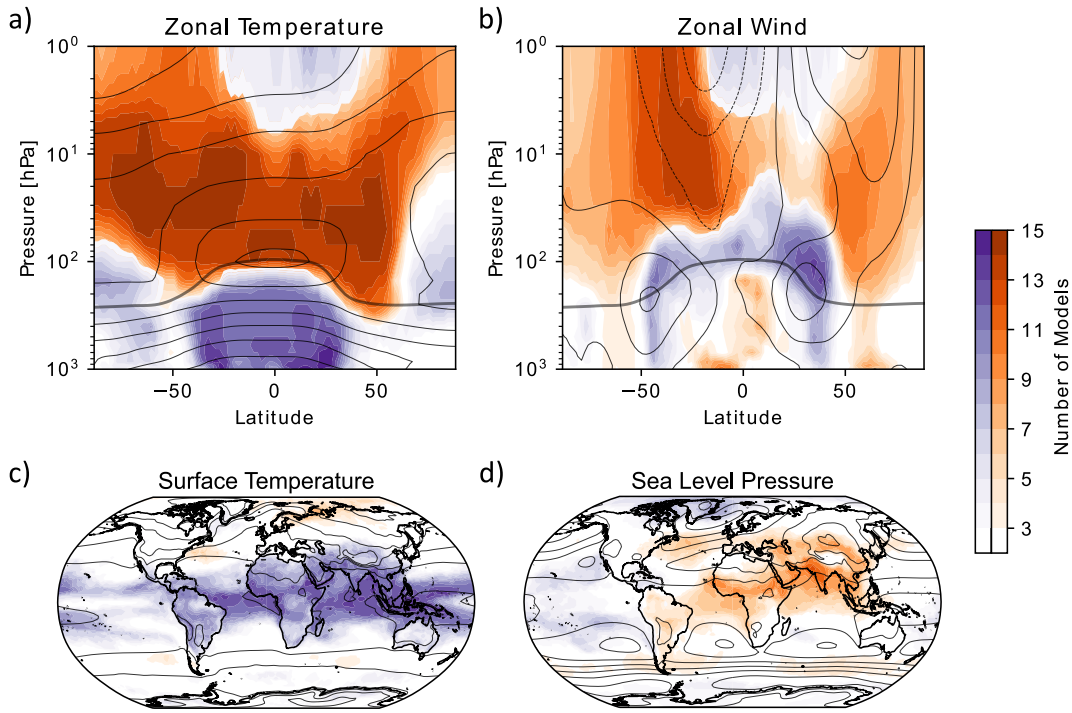

Figure 3. Number of Models showing a significant anomaly to the Pinatubo + Krakatoa eruption. Shown are the numbers of models with a significant increase (orange) or decrease (purple) in winter after the Krakatoa and Pinatubo eruption for (a) mean zonal temperature, (b) zonal mean zonal wind, (c) mean surface temperature, and (d) mean sea level pressure. Areas with less than three models showing a significant anomaly are white. The significance is computed with a one-sided *t*-test at a 95% level. The contours show the composite means for the five winters before the eruption with (a) 15K, (b) 15 m^{-1}, (c) 10K, (d) 6 hPa increments. The mean topopause height from CNRM-ESM2-1, IPSL-CM6A-LR, UKESM1-0-LL, GISS-E2-1-G and CESM2 for NH winter 1986–1991 is marked with a thick gray line in panels (a, b).

winter atmosphere masks the volcanic signal. The analysis of the large ensemble of the CMIP6 historical experiment and the variability between the individual ensemble members suggests that the observed and postulated stratospheric pathway is reproduced in the CMIP6 models for the two strongest eruptions in the historical period. However, the large NH winter variability in temperatures and winds also allows for results that are weaker or opposite to those observed in the 20th century. Large numbers of simulations and care about the choice for spatial averaging are required to separate the forced volcanic response from internal variability.

In contrast to the NAO-phase, we find no dependence on ENSO for the winter response to volcanic forcing (Figures 4e–4h). In addition, the CMIP6 output shows no clear dependence of the response to volcanic forcing on the ENSO phase before the eruption (Figure S6 in Supporting Information S1). Coupe and Robock (2021) suggested that the coexistence for a positive ENSO phase is needed in order to simulate the surface winter warming in Europe, whereas Dogar et al. (2024) found no need for a positive ENSO phase to simulate the positive NAO phase for one model. Correspondingly, the CMIP6 multi-model mean responses of the near-surface temperature in Europe and the polar vortex strength are independent of the ENSO phase during both the preceding and the following post-eruption winters (Figure 4 and Figure S3 in Supporting Information S1). This is not surprising given the large variability of observed ENSO with stratospheric polar winter and spring responses after volcanic eruptions (Domeisen et al., 2019; Garfinkel et al., 2012; Labitzke & Loon, 1989; Van Loon & Labitzke, 1987). Also the quasi-biennial oscillation (QBO) may impact the volcanic aerosol forcing and climate response (Labitzke & Loon, 1989; Thomas, Giorgetta, et al., 2009; Thomas, Timmreck, et al., 2009; Van Loon & Labitzke, 1987; Zhuo et al., 2024). As Butchart et al. (2023) pointed out, the QBO-phase is synchronized across historical experiments due to the CMIP6 prescribed ozone forcings, inhibiting an analysis of the influence of the QBO on the volcanically induced climate responses in the historical experiments. It might be interesting to analyse the role of modes of climate variability and responses in other world regions with other model experiments, for example, in the context of VolMIP (Zanchettin et al., 2016, 2022).

10.1029/2025GL120522

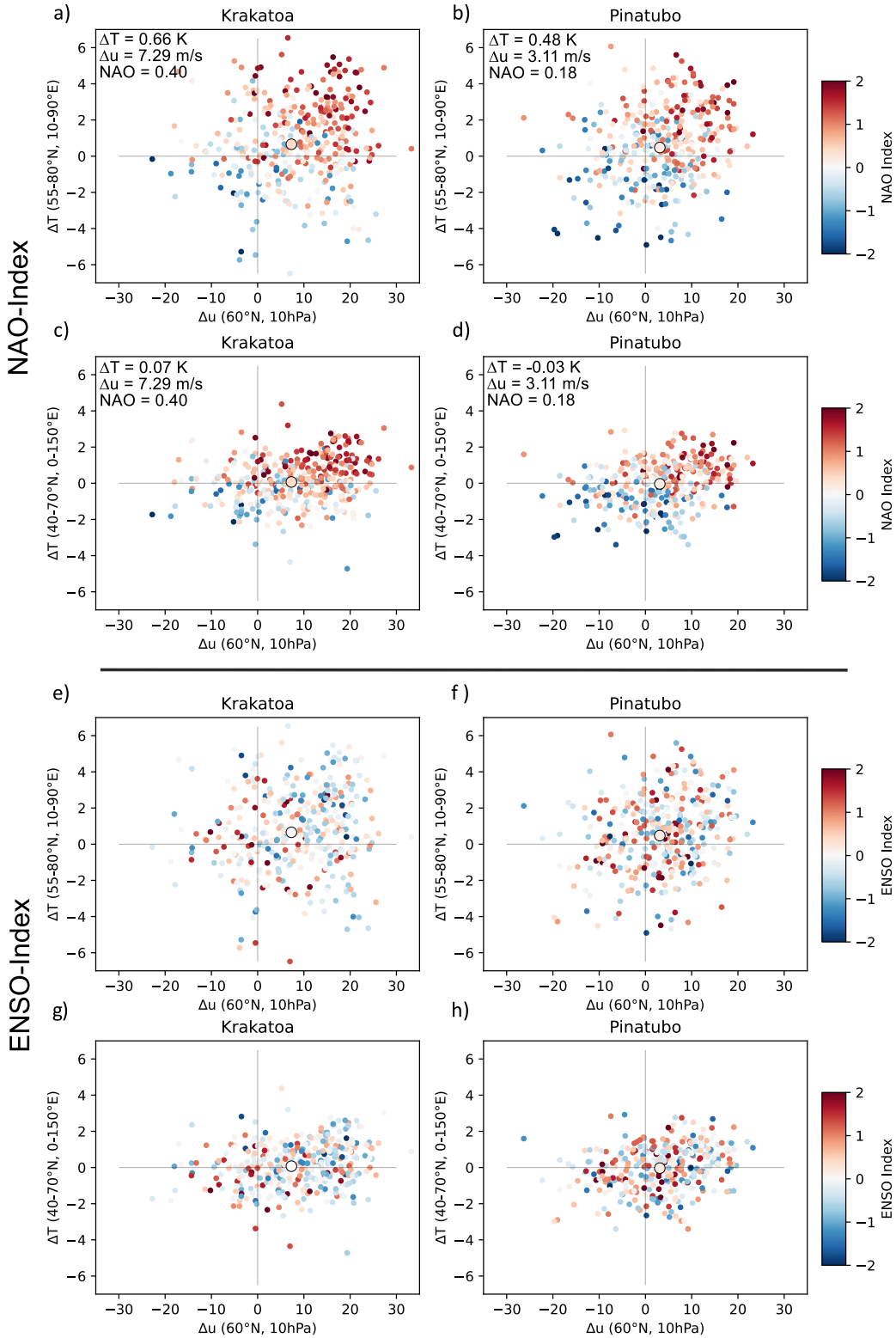

Figure 4. Response of the zonal wind (Δu) in the polar vortex against surface temperature (ΔT) during the first winter (DJF) following the volcanic eruptions relative to the mean over the five winters before the eruption. Each dot refers to the response simulated by an individual model experiment and is color-coded by the (a–d) NAO-Index and (e–h) ENSO-Index (Oceanic Niño Index) during the post-eruption winter computed on relative SST anomalies. Larger circles mark the multi-model CMIP6 means. Results are for (a, b, e, f) ΔT in the region 55–80°N and 10–90°E (Azoulay et al., 2021) and (c, d, g, h) in Eurasia for 40–70°N and 0–150°E (Polvani & Camargo, 2020).

4. Conclusion

We address the climate response in NH winter after the two largest volcanic eruptions in the historical period, Krakatoa 1883 and Pinatubo 1991. Our analysis uses historical experiments from 15 CMIP6 models with more than 10 individual simulations each and three reanalysis data sets. In the CMIP6 multi-model mean, the post-eruption winters show stronger winds in the polar vortex and near-surface warming across Northern Eurasia. Internal variability strongly affects these responses, underlining the need for large ensembles to study the response of dynamical processes to forcing.

We identify also a positive NAO independent of ENSO in the CMIP6 mean over the simulated post-eruption winter, with large variability across individual historical experiment. Moreover, the magnitude of the near-surface temperature response in Eurasia is sensitive to the region for spatial averaging. These results explain some disagreements between previous studies on addressing the climate responses to volcanic forcing. A different spatial pattern in reanalysis data or even the absence of a strong surface warming in single model realizations is no contradiction to the fact that strong low-latitude volcanic forcing favors a near-surface winter warming, as shown by the CMIP6 multi-model mean in our results. Any model differences in surface winter warming patterns and strengths following major volcanic eruptions rather supports the finding that the large interannual variability in the NH influences and potentially suppresses marked surface signatures following even the strongest volcanic eruptions witnessed between 1850 and today. Separating the forced response from internal variability for volcanic eruptions therefore requires a strong volcanic forcing and a large number of simulations in addition to carefully designed data analyses for the dynamical processes at play.

Conflict of Interest

The authors declare no conflicts of interest relevant to this study.

Availability Statement

The used CMIP6 output and reanalyses data, listed in Tables S1 and S2 of Supporting Information S1, are freely available. CMIP6 output are available via the Earth System Grid Federation (https://esgf-data.dkrz.de/search/cmip6-dkrz/), ERA5 reanalysis of the European Center for Medium-Range Weather Forecasts (ERA5, 2025) is provided through the Copernicus Climate Change Service (C3S) Data Store (CDS, 2025), the Japanese 55-year Reanalysis (JRA-55) is provided by the Japan Meteorological Agency (JMA, 2025), and the NOAA/CIRES/DOE 20th Century Reanalysis (V3) data is provided by the National Oceanic and Atmospheric Administration's Physical Sciences Laboratory (https://www.psl.noaa.gov/data/gridded/data.20thC_ReanV3.html).

Acknowledgments

This work used resources of the Deutsches Klimarechenzentrum (DKRZ) Granted by its Scientific Steering Committee (WLA) under project ID bb1198 for supporting research on aerosol-circulation interactions. KK acknowledges support by the University of Oslo Energy and Environment Convergence Environment project "ClimSHOCK", the Centre for Advanced Study "NORLIA" project and the RCN project "NorESM4CMIP7" (Grant 352204). SF is supported by the European Union's HORIZON project EXPECT (No.: 101137656 HORIZON-CL5-2023-D1-01) and the Deutsche Forschungsgemeinschaft (DFG, German Research Foundation) via project DETECT (SFB 1502/1–2022 - Projektnummer: 450058266). LW acknowledges the Erasmus + Traineeship support for a research visit at the University of Oslo. We acknowledge the CMIP6 community for providing the climate model output, retained and globally distributed via the ESGF. Open Access funding enabled and organized by Projekt DEAL.

References

Azoulay, A., Schmidt, H., & Timmreck, C. (2021). The Arctic polar vortex response to volcanic forcing of different strengths. *Journal of Geophysical Research: Atmospheres*, *126*(11), e2020JD034450. https://doi.org/10.1029/2020JD034450

Bethke, I., Wang, Y., Counillon, F., Keenlyside, N., Kimmritz, M., Fransner, F., et al. (2021). NorCPM1 and its contribution to CMIP6 DCPP. *Geoscientific Model Development*, *14*(11), 7073–7116. https://doi.org/10.5194/gmd-14-7073-2021

Bittner, M., Schmidt, H., Timmreck, C., & Sienz, F. (2016). Using a large ensemble of simulations to assess the Northern Hemisphere stratospheric dynamical response to tropical volcanic eruptions and its uncertainty. *Geophysical Research Letters*, *43*(17), 9324–9332. https://doi.org/10.1002/2016GL070587

Bittner, M., Timmreck, C., Schmidt, H., Toohey, M., & Krüger, K. (2016). The impact of wave-mean flow interaction on the Northern Hemisphere polar vortex after tropical volcanic eruptions. *Journal of Geophysical Research: Atmospheres*, *121*(10), 5281–5297. https://doi.org/10.1002/2015JD024603

Butchart, N., Andrews, M. B., & Jones, C. D. (2023). QBO phase synchronization in CMIP6 historical simulations attributed to ozone forcing. *Geophysical Research Letters*, *50*(15), e2023GL104401. https://doi.org/10.1029/2023GL104401

CDS. (2025). Complete ERA5 global atmospheric reanalysis [Dataset]. *Copernicus Climate Change Service (C3S) Climate Data Store (CDS)*. https://doi.org/10.24381/cds.143582cf

Charlton-Perez, A. J., Baldwin, M. P., Birner, T., Black, R. X., Butler, A. H., Calvo, N., et al. (2013). On the lack of stratospheric dynamical variability in low-top versions of the CMIP5 models. *Journal of Geophysical Research: Atmospheres*, *118*(6), 2494–2505. https://doi.org/10.1002/jgrd.50125

Coupe, J., & Robock, A. (2021). The influence of stratospheric soot and sulfate aerosols on the Northern Hemisphere wintertime atmospheric circulation. *Journal of Geophysical Research: Atmospheres*, *126*(11), e2020JD034513. https://doi.org/10.1029/2020JD034513

Dawson, A. (2016). eofs: A library for EOF analysis of meteorological, oceanographic, and climate data. *Journal of Open Research Software*, *4*(1), 14. https://doi.org/10.5334/jors.122

Dogar, M. M., Fujiwara, M., Zhao, M., Ohba, M., & Kosaka, Y. (2024). ENSO and NAO linkage to strong volcanism and associated post-volcanic high-latitude winter warming. *Geophysical Research Letters*, *51*(1), e2023GL106114. https://doi.org/10.1029/2023GL106114

Domeisen, D. I., Garfinkel, C. I., & Butler, A. H. (2019). The teleconnection of El Niño Southern oscillation to the stratosphere. *Reviews of Geophysics*, *57*(1), 5–47. https://doi.org/10.1029/2018RG000596

Döscher, R., Acosta, M., Alessandri, A., Anthoni, P., Arsouze, T., Bergman, T., et al. (2022). The EC-Earth3 Earth system model for the Coupled Model Intercomparison Project 6. *Geoscientific Model Development*, *15*(7), 2973–3020. https://doi.org/10.5194/gmd-15-2973-2022

Driscoll, S., Bozzo, A., Gray, L. J., Robock, A., & Stenchikov, G. (2012). Coupled Model Intercomparison Project 5 (CMIP5) simulations of climate following volcanic eruptions. *Journal of Geophysical Research*, *117*(D17), 2012JD017607. https://doi.org/10.1029/2012JD017607

ERA5, Hersbach, H., Bell, B., Berrisford, P., Hirahara, S., Horányi, A., et al. (2025). Complete ERA5 from 1940: Fifth generation of ECMWF atmospheric reanalyses of the global climate [Dataset]. *Copernicus Climate Change Service (C3S) Data Store (CDS)*. https://doi.org/10.24381/cds.143582cf

Garfinkel, C. I., Butler, A. H., Waugh, D. W., Hurwitz, M. M., & Polvani, L. M. (2012). Why might stratospheric sudden warmings occur with similar frequency in El Niño and La Niña winters? *Journal of Geophysical Research*, *117*(D19), 2012JD017777. https://doi.org/10.1029/2012JD017777

Graf, H.-F., Zanchettin, D., Timmreck, C., & Bittner, M. (2014). Observational constraints on the tropospheric and near-surface winter signature of the Northern Hemisphere stratospheric polar vortex. *Climate Dynamics*, *43*(12), 3245–3266. https://doi.org/10.1007/s00382-014-2101-0

Hajima, T., Watanabe, M., Yamamoto, A., Tatebe, H., Noguchi, M. A., Abe, M., et al. (2020). Development of the MIROC-ES2L Earth system model and the evaluation of biogeochemical processes and feedbacks. *Geoscientific Model Development*, *13*(5), 2197–2244. https://doi.org/10.5194/gmd-13-2197-2020

Hersbach, H., Bell, B., Berrisford, P., Hirahara, S., Horányi, A., Muñoz-Sabater, J., et al. (2020). The ERA5 global reanalysis. *Quarterly Journal of the Royal Meteorological Society*, *146*(730), 1999–2049. https://doi.org/10.1002/qj.3803

Hourdin, F., Rio, C., Grandpeix, J., Madeleine, J., Cheruy, F., Rochetin, N., et al. (2020). LMDZ6A: The atmospheric component of the IPSL climate model with improved and better tuned physics. *Journal of Advances in Modeling Earth Systems*, *12*(7), e2019MS001892. https://doi.org/10.1029/2019MS001892

Hurrell, J. W., Kushnir, Y., Ottersen, G., & Visbeck, M. (2003). An overview of the North Atlantic Oscillation. In J. W. Hurrell, Y. Kushnir, G. Ottersen, & M. Visbeck (Eds.), *Geophysical monograph series* (Vol. 134, pp. 1–35). American Geophysical Union. https://doi.org/10.1029/134GM01

JMA. (2025). JRA-55: Japanese 55-year reanalysis, daily 3-Hourly and 6-Hourly data [Dataset]. *NSF National Center for Atmospheric Research, Japan Meteorological Agency, Japan*. https://doi.org/10.5065/D6HH6H41

Jones, P. W. (1999). First- and second-order conservative remapping schemes for grids in spherical coordinates. *Monthly Weather Review*, *127*(9), 2204–2210. https://doi.org/10.1175/1520-0493(1999)127⟨2204:FASOCR⟩2.0.CO;2

Khodri, M., Izumo, T., Vialard, J., Janicot, S., Cassou, C., Lengaigne, M., et al. (2017). Tropical explosive volcanic eruptions can trigger El Niño by cooling tropical Africa. *Nature Communications*, *8*(1), 778. https://doi.org/10.1038/s41467-017-00755-6

Kobayashi, S., Ota, Y., Harada, Y., Ebita, A., Moriya, M., Onoda, H., et al. (2015). The JRA-55 reanalysis: General specifications and basic characteristics. *Journal of the Meteorological Society of Japan. Series II*, *93*(1), 5–48. https://doi.org/10.2151/jmsj.2015-001

Krüger, K., Langematz, U., Grenfell, J., & Labitzke, K. (2005). Climatological features of stratospheric streamers in the FUB-CMAM with increased horizontal resolution. *Atmospheric Chemistry and Physics*, *5*(2), 547–562. https://doi.org/10.5194/acp-5-547-2005

Labitzke, K. (1982). On the interannual variability of the middle stratosphere during the Northern winters. *Journal of the Meteorological Society of Japan. Series II*, *60*(1), 124–139. https://doi.org/10.2151/jmsj1965.60.1_124

Labitzke, K., & Loon, H. (1989). The Southern oscillation. Part IX: The influence of volcanic eruptions on the Southern oscillation in the stratosphere. *Journal of Climate*, *2*(10), 1223–1226. https://doi.org/10.1175/1520-0442(1989)002⟨1223:TSOPIT⟩2.0.CO;2

Labitzke, K., & Van Loon, H. (1999). *The stratosphere*. Springer Berlin Heidelberg. https://doi.org/10.1007/978-3-642-58541-8

Mauritsen, T., Bader, J., Becker, T., Behrens, J., Bittner, M., Brokopf, R., et al. (2019). Developments in the MPI-M Earth System Model version 1.2 (MPI-ESM1.2) and its response to increasing CO_2. *Journal of Advances in Modeling Earth Systems*, *11*(4), 998–1038. https://doi.org/10.1029/2018MS001400

Meehl, G. A., Arblaster, J. M., Bates, S., Richter, J. H., Tebaldi, C., Gettelman, A., et al. (2020). Characteristics of future warmer base states in CESM2. *Earth and Space Science*, *7*(9), e2020EA001296. https://doi.org/10.1029/2020EA001296

Metzner, D., Kutterolf, S., Toohey, M., Timmreck, C., Niemeier, U., Freundt, A., & Krüger, K. (2014). Radiative forcing and climate impact resulting from so 2 injections based on a 200,000-year record of Plinian eruptions along the Central American Volcanic Arc. *International Journal of Earth Sciences*, *103*(7), 2063–2079. https://doi.org/10.1007/s00531-012-0814-z

Miller, R. L., Schmidt, G. A., Nazarenko, L. S., Bauer, S. E., Kelley, M., Ruedy, R., et al. (2021). CMIP6 historical simulations (1850–2014) with GISS-E2.1. *Journal of Advances in Modeling Earth Systems*, *13*(1), e2019MS002034. https://doi.org/10.1029/2019MS002034

Müller, W. A., Jungclaus, J. H., Mauritsen, T., Baehr, J., Bittner, M., Budich, R., et al. (2018). A higher-resolution version of the Max Planck Institute Earth System model (MPI-ESM1.2-HR). *Journal of Advances in Modeling Earth Systems*, *10*(7), 1383–1413. https://doi.org/10.1029/2017MS001217

Paik, S., Min, S.-K., Son, S.-W., Lim, E.-P., McGregor, S., An, S.-I., et al. (2023). Impact of volcanic eruptions on extratropical atmospheric circulations: Review, revisit and future directions. *Environmental Research Letters*, *18*(6), 063003. https://doi.org/10.1088/1748-9326/acd5e6

Pauling, A. G., Bitz, C. M., & Armour, K. C. (2023). The climate response to the Mt. Pinatubo eruption does not constrain climate sensitivity. *Geophysical Research Letters*, *50*(7), e2023GL102946. https://doi.org/10.1029/2023GL102946

Poberaj, C. S., Staehelin, J., & Brunner, D. (2011). Missing stratospheric ozone decrease at Southern Hemisphere middle latitudes after Mt. Pinatubo: A dynamical perspective. *Journal of the Atmospheric Sciences*, *68*(9), 1922–1945. https://doi.org/10.1175/JAS-D-10-05004.1

Polvani, L. M., Banerjee, A., & Schmidt, A. (2019). Northern Hemisphere continental winter warming following the 1991 Mt. Pinatubo eruption: Reconciling models and observations. *Atmospheric Chemistry and Physics*, *19*(9), 6351–6366. https://doi.org/10.5194/acp-19-6351-2019

Polvani, L. M., & Camargo, S. J. (2020). Scant evidence for a volcanically forced winter warming over Eurasia following the Krakatau eruption of August 1883. *Atmospheric Chemistry and Physics*, *20*(22), 13687–13700. https://doi.org/10.5194/acp-20-13687-2020

Rao, J., Garfinkel, C. I., Wu, T., Lu, Y., & Chu, M. (2022). Mean state of the Northern Hemisphere stratospheric polar vortex in three generations of CMIP models. *Journal of Climate*, *35*(14), 4603–4625. https://doi.org/10.1175/JCLI-D-21-0694.1

Robock, A. (2000). Volcanic eruptions and climate. *Reviews of Geophysics*, *38*(2), 191–219. https://doi.org/10.1029/1998RG000054

Robock, A., & Mao, J. (1992). Winter warming from large volcanic eruptions. *Geophysical Research Letters*, *19*(24), 2405–2408. https://doi.org/10.1029/92GL02627

Robock, A., & Mao, J. (1995). The volcanic signal in surface temperature observations. *Journal of Climate*, *8*(5), 1086–1103. https://doi.org/10.1175/1520-0442(1995)008⟨1086:TVSIST⟩2.0.CO;2

Schemm, S. (2023). Toward eliminating the decades-old "too zonal and too equatorward" storm-track bias in climate models. *Journal of Advances in Modeling Earth Systems*, *15*(2), e2022MS003482. https://doi.org/10.1029/2022MS003482

Schmidt, A., & Black, B. A. (2022). Reckoning with the rocky relationship between eruption size and climate response: Toward a volcano-climate index. *Annual Review of Earth and Planetary Sciences*, *50*(1), 627–661. https://doi.org/10.1146/annurev-earth-080921-052816

Séférian, R., Nabat, P., Michou, M., Saint-Martin, D., Voldoire, A., Colin, J., et al. (2019). Evaluation of CNRM Earth System Model, CNRM-ESM2-1: Role of Earth System processes in present-day and future climate. *Journal of Advances in Modeling Earth Systems*, *11*(12), 4182–4227. https://doi.org/10.1029/2019MS001791

Sellar, A. A., Jones, C. G., Mulcahy, J. P., Tang, Y., Yool, A., Wiltshire, A., et al. (2019). UKESM1: Description and evaluation of the U.K. Earth System model. *Journal of Advances in Modeling Earth Systems*, *11*(12), 4513–4558. https://doi.org/10.1029/2019MS001739

Slivinski, L. C., Compo, G. P., Whitaker, J. S., Sardeshmukh, P. D., Giese, B. S., McColl, C., et al. (2019). Towards a more reliable historical reanalysis: Improvements for version 3 of the Twentieth Century Reanalysis system. *Quarterly Journal of the Royal Meteorological Society*, *145*(724), 2876–2908. https://doi.org/10.1002/qj.3598

Stenchikov, G., Hamilton, K., Stouffer, R. J., Robock, A., Ramaswamy, V., Santer, B., & Graf, H. (2006). Arctic Oscillation response to volcanic eruptions in the IPCC AR4 climate models. *Journal of Geophysical Research*, *111*(D7), 2005JD006286. https://doi.org/10.1029/2005JD006286

Stenchikov, G., Robock, A., Ramaswamy, V., Schwarzkopf, M. D., Hamilton, K., & Ramachandran, S. (2002). Arctic Oscillation response to the 1991 Mount Pinatubo eruption: Effects of volcanic aerosols and ozone depletion. *Journal of Geophysical Research*, *107*(D24). https://doi.org/10.1029/2002JD002090

Swart, N. C., Cole, J. N. S., Kharin, V. V., Lazare, M., Scinocca, J. F., Gillett, N. P., et al. (2019). The Canadian Earth System Model version 5 (CanESM5.0.3). *Geoscientific Model Development*, *12*(11), 4823–4873. https://doi.org/10.5194/gmd-12-4823-2019

Tatebe, H., Ogura, T., Nitta, T., Komuro, Y., Ogochi, K., Takemura, T., et al. (2019). Description and basic evaluation of simulated mean state, internal variability, and climate sensitivity in MIROC6. *Geoscientific Model Development*, *12*(7), 2727–2765. https://doi.org/10.5194/gmd-12-2727-2019

Thomas, M. A., Giorgetta, M. A., Timmreck, C., Graf, H.-F., & Stenchikov, G. (2009). Simulation of the climate impact of Mt. Pinatubo eruption using ECHAM5 – Part 2: Sensitivity to the phase of the QBO and ENSO. *Atmospheric Chemistry and Physics*, *9*(9), 3001–3009. https://doi.org/10.5194/acp-9-3001-2009

Thomas, M. A., Timmreck, C., Giorgetta, M. A., Graf, H.-F., & Stenchikov, G. (2009). Simulation of the climate impact of Mt. Pinatubo eruption using ECHAM5 – Part 1: Sensitivity to the modes of atmospheric circulation and boundary conditions. *Atmospheric Chemistry and Physics*, *9*(2), 757–769. https://doi.org/10.5194/acp-9-757-2009

Thomason, L. W., Ernest, N., Millán, L., Rieger, L., Bourassa, A., Vernier, J.-P., et al. (2018). A global space-based stratospheric aerosol climatology: 1979–2016. *Earth System Science Data*, *10*(1), 469–492. https://doi.org/10.5194/essd-10-469-2018

Toohey, M., Krüger, K., Bittner, M., Timmreck, C., & Schmidt, H. (2014). The impact of volcanic aerosol on the Northern Hemisphere stratospheric polar vortex: Mechanisms and sensitivity to forcing structure. *Atmospheric Chemistry and Physics*, *14*(23), 13063–13079. https://doi.org/10.5194/acp-14-13063-2014

Van Loon, H., & Labitzke, K. (1987). The Southern oscillation. Part V: The anomalies in the lower stratosphere of the Northern Hemisphere in Winter and a comparison with the quasi-biennial oscillation. *Monthly Weather Review*, *115*(2), 357–369. https://doi.org/10.1175/1520-0493(1987)115⟨0357:TSOPVT⟩2.0.CO;2

Vecchi, G. A., & Soden, B. J. (2007). Effect of remote sea surface temperature change on tropical cyclone potential intensity. *Nature*, *450*(7172), 1066–1070. https://doi.org/10.1038/nature06423

Voldoire, A., Saint-Martin, D., Sénési, S., Decharme, B., Alias, A., Chevallier, M., et al. (2019). Evaluation of CMIP6 DECK experiments with CNRM-CM6-1. *Journal of Advances in Modeling Earth Systems*, *11*(7), 2177–2213. https://doi.org/10.1029/2019MS001683

Volodin, E. M., Mortikov, E. V., Kostrykin, S. V., Galin, V. Y., Lykosov, V. N., Gritsun, A. S., et al. (2017). Simulation of modern climate with the new version of the INM RAS climate model. *Izvestiya - Atmospheric and Oceanic Physics*, *53*(2), 142–155. https://doi.org/10.1134/S0001433817020128

Zambri, B., & Robock, A. (2016). Winter warming and summer monsoon reduction after volcanic eruptions in Coupled Model Intercomparison Project 5 (CMIP5) simulations. *Geophysical Research Letters*, *43*(20). https://doi.org/10.1002/2016GL070460

Zanchettin, D., Khodri, M., Timmreck, C., Toohey, M., Schmidt, A., Gerber, E. P., et al. (2016). The Model Intercomparison Project on the climatic response to Volcanic forcing (VolMIP): Experimental design and forcing input data for CMIP6. *Geoscientific Model Development*, *9*(8), 2701–2719. https://doi.org/10.5194/gmd-9-2701-2016

Zanchettin, D., Timmreck, C., Khodri, M., Schmidt, A., Toohey, M., Abe, M., et al. (2022). Effects of forcing differences and initial conditions on inter-model agreement in the VolMIP volc-pinatubo-full experiment. *Geoscientific Model Development*, *15*(5), 2265–2292. https://doi.org/10.5194/gmd-15-2265-2022

Zhuo, Z., Fuglestvedt, H. F., Toohey, M., & Krüger, K. (2024). Initial atmospheric conditions control transport of volcanic volatiles, forcing and impacts. *Atmospheric Chemistry and Physics*, *24*(10), 6233–6249. https://doi.org/10.5194/acp-24-6233-2024

Ziehn, T., Chamberlain, M. A., Law, R. M., Lenton, A., Bodman, R. W., Dix, M., et al. (2020). The Australian Earth System model: ACCESS-ESM1.5. *Journal of Southern Hemisphere Earth Systems Science*, *70*(1), 193–214. https://doi.org/10.1071/ES19035